Temperature Dependent Characteristics of DH36 Steel Fatigue Crack Propagation

Weidong Zhao[1], Guoqing Feng[1*], Huilong Ren[1], Bernt Johan Leira[2], Ming Zhang[1],

1.Harbin Engineering University. Harbin, P. R. China

2. Norwegian University of Science and Technology. Trondheim, Norway

Correspondence to: Guoqing Feng. E-mail: fengguoqing@hrbeu.edu.cn

Abstract

DH36 steel is a widely used material in marine engineering. The fatigue crack propagation rates of DH36 steel at low temperatures has a crucial influence on the fatigue strength of structures operating in polar environments. The objective of this paper is to investigate the fatigue crack propagation behavior of DH36 steel at low temperatures (-60℃~20℃) by carrying out tensile tests and fatigue crack propagation tests of DH36 steel, in order to obtain the fatigue crack propagation behavior of DH36 steel. The influence of the elastic modulus on the crack length measured by the compliance method is considered. Based on the Paris law, the crack propagation rate at different temperatures is investigated. The results and the observed failure modes indicated that Fatigue Ductile to Brittle Transition (FDBT) occurred as the temperature was lowered.

Keywords: DH36 steel; fatigue crack propagation; low temperatures; failure mode; FDBT.

Nomenclature

a	length of the crack
B	thickness of the specimen
C , m	crack propagation parameters
DBTT	Ductile to Brittle Transition Temperature

da/dN	the fatigue crack propagation rate
E	the elastic modulus
FDBT	Fatigue Ductile to Brittle Transition
FTT	Fatigue Transition Temperature
N	number of cycles
P	load
ΔP	load range
T	temperature
T_0	temperature at which the K_{Ic} is 100MPa$\sqrt{\text{m}}$
T_{27J}	temperature at which the Charpy impact energy is 27J (℃).
U_0	compliance at the measuring point
V_0	displacement measured by the displacement gauge
W	width of specimen
α	crack depth ratio a/W
ΔK	stress intensity factor range
K_{IC}	critical stress intensity factor for mode I (MPa$\sqrt{\text{m}}$)

1. Introduction

There has been a considerable increase in the use of high strength steels in offshore structures and polar ship hulls. These structures experience millions of load cycles in service and are also exposed to harsh marine environments that may result in fatigue failures [1]. Once microcracks occur in these structures, they will continue to expand until the structures fail under alternating loads [2]. Therefore, microcracks have become a serious concern as they pose a great threat to the safety of such structures in polar regions.

There are two major approaches for analysis of fatigue strength: the S-N Curve Approach and the Fracture Mechanics Approach [3]. Compared with the S-N Curves Approach, the Fracture Mechanics Approach takes into account the microcracks which exist already at the initial state of the structure. By this means, the Fracture Mechanics Approach provides a fracture criterion for the crack-containing body while the S-N Curves Approach does not represent the cracks explictly. Therefore, the Fracture Mechanics Approach is more appropriate for the purpose of the present paper. The Fracture Mechanics Approach falls into two categories: The Linear Elastic Fracture Mechanics and the Elastoplastic Fracture Mechanics Approaches, respectively. Despite the rapid development of the Elastoplastic Fracture Mechanics Approach, the Linear Elastic Fracture Mechanics Approach still plays a crucial role in design against fatigue. The Linear Elastic Fracture Mechanics Approach is suitable for small-scale yielding near the crack tip, while the Elastoplastic Fracture Mechanics Approach is more suitable for large-scale yielding near the crack tip. The state of the crack tip in this paper belongs to small-scale yielding, and accordingly the Linear Elastic Fracture Mechanics Approach is adopted to study the effect of low temperatures on the fatigue crack propagation rates in this paper.

Based on the Linear Elastic Fracture Mechanics Approach, a series of corresponding design procedures [4-7] have been developed for fatigue-prone structural details in order to evaluate the fatigue performances of polar ships and other welded steel structures [8,9]. However, most of these studies only focused on the crack growth parameters in Paris law at room temperature, and the data used to estimate these parameters came primarily from experimental data which were recorded at room temperature. The validity of these parameters at low ambient temperature requires further validation for the purpose of enhanced fatigue assessment of polar ships. Previous studies have examined the fatigue crack propagation behavior of structural steels experimentally, including Q345qD, Fe25Mn and Fe16Mn2Al steels [10,11]. Liao studied fatigue crack propagation behavior of Q345qD bridge steel base metal as well as the butt welds. Their results demonstrated a reduced fatigue crack propagation rate in the base metal as the ambient temperature was lowered [10]. Fassina studied the

influence of low temperature on fatigue crack growth properties of two pipeline materials, i.e. micro-alloyed X65 and F22 low alloy steels [12]. However, the steel they studied has not been widely applied in polar ship hulls.

For ships operating in low temperature environments, the open deck plating, side slabs above cold water line (CWL), and transverse bulkheads above CWL are of grade I [13], as shown in Table 1. It reveals that the study of fatigue crack propagation rates of DH36 steel at -60℃~20℃ has great practical significance for the evaluation of fatigue crack propagation of polar ships. A similar specification is given in the "Ships for navigation in ice" published by Det Norske Veritas (DNV) [14]. However, there has been limited research on the fatigue crack propagation rates of DH36 steel in low temperature environment. Therefore, the fatigue crack propagation performance of DH36 steel commonly used in polar ships under low temperature remain to be studied.

Table1 Steel grade required for material grade I in low temperature environment

t /mm	Design service temperature(℃)											
	-23~-27℃		-28~-32℃		-33~-38℃		-39~-48℃		-49~58℃		-59~-68℃	
	MS	HT	MS	HT	MS	HT	MS	HT	MS	HT	MS	HT
$t \leq 10$	A	AH	A	AH	B	AH	B	AH	D	DH	D	DH
$10 < t \leq 15$	A	AH	A	AH	B	AH	D	DH	D	DH	D	DH
$15 < t \leq 20$	B	AH	B	AH	B	AH	D	DH	D	DH	E	EH
$20 < t \leq 25$	B	AH	B	AH	D	DH	D	DH	D	DH	E	EH
$25 < t \leq 30$	B	AH	D	DH	D	DH	D	DH	E	EH	E	EH
$30 < t \leq 35$	D	DH	D	DH	D	DH	D	DH	E	EH	E	EH
$35 < t \leq 45$	D	DH	D	DH	D	DH	E	EH	E	EH	-	FH
$45 < t \leq 50$	D	DH	D	DH	E	EH	E	EH	-	EH	-	FH

Where, t is the thickness of steels, MS is Mild steel, HT is High strength steel.

The structural steel for hull is grouped into general thickness and high strength steel. General strength steel is graded into four categories according to quality: A, B, C and D; high strength steel is divided into two strength grades and three quality grades: AH32, DH32, EH32, AH36, DH36, EH36.

The objective of the present paper is to investigate the effect of low temperatures on the fatigue crack propagation behavior of DH36 steel. Based on the experiment results, this study seeks to recommend corresponding Paris-law crack-growth parameters for the fatigue crack behavior of DH36 steel at -60℃~20℃. Post-testing fractography was performed by means of a scanning electron microscope (SEM) in order to understand the underlying mechanism responsible for the observed fracture modes. This study first presents the material properties and the experimental details in section 2 and section 3. Section 4 presents a microstructural characterization as well as results for the fatigue crack propagation and the fracture modes of DH36 steel at -60℃~20℃. Section 5 summarizes the main conclusions of the study.

2. Tensile tests

The fatigue crack growth properties of metallic material are closely related to tensile properties: the elastic modulus of the metallic material can affect the measurement accuracy of the crack length when the crack length is measured by the compliance method. Generally, the elastic modulus of metallic material changes with temperature. Therefore, the tensile test was carried out under low temperature in this paper before the fatigue crack propagation test was carried out.

2.1 Tensile test specimens

The material used for the low temperature tensile tests is DH36 steel which is certified by the American Bureau of Shipping (ABS). The chemical composition of DH36 steel is shown in Table 2. The specimens (Fig. 1) were designed and manufactured according to GB/T 13239-2006 “Metal Material-Tensile Testing at Low Temperature” [15].

Table 2 Chemical Compositions of DH36 steel

	Chemical compositions, %						
DH36	C	Si	Mn	P	S	Als	Cr
	0.17	0.20	1.16	0.018	0.0034	0.023	0.02
	Nb	V	Ti	Mo	Ni	Cu	Ceq

	0.015	0.002	0.017	0	0.01	0.02	0.37

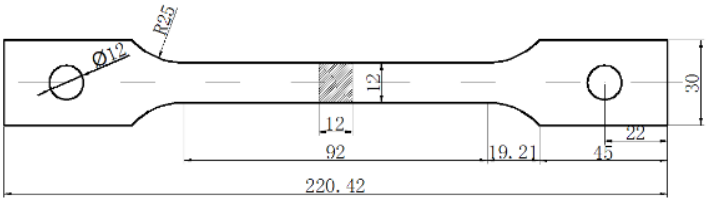

(a) Schematic diagram

(b) Physical realization of a specimen

Fig. 1 Tensile specimen

2.2 Test equipment

A low temperature chamber that compresses air to achieve a cold environment during the test was used, as shown in Fig. 2. Refrigeration by air compression allows easier operation and produces more stable temperatures than refrigeration by liquid nitrogen within the range from -70℃ to 20℃. To guarantee a stable low temperature environment, an industrial thermometer was placed in the chamber so that the internal temperature could be periodically monitored.

Fig. 2 Low temperature test device

A PWS-250 fatigue machine having a displacement rate with an accuracy of

3×10^{-5} m/s and which can produce a maximum static load of 25t was applied for the tensile test. A YYU-±40/50 high-precision low temperature extensometer with a gauge length of 50 mm and a deformation of 40 mm was adopted.

2.3 Test program and results

First, the specimen was installed as shown in Fig. 3(a). Then, the low temperature chamber was activated in order to produce the selected test temperatures (respectively 20℃, 0℃, -20℃, -40℃ and -60℃). A test duration of 20 minutes was applied after the specified experimental temperature was reached. During this time, reading of the extensometer was performed and the channels were balanced to eliminate errors caused by temperature drift. Each specimen was stretched until fracture based on the strain controlled mode took place (Fig. 3(b)). The tensile test was repeated 5 times at each test temperature to ensure the validity of the data. The yield strength and the elastic modulus at each temperature were obtained by data processing with the results shown in Fig. 4. It can be seen that the yield strength decreases as temperature increases; the elastic modulus also exhibits a similar tendency.

(a) Installation of specimen in the low temperature chamber

(b) Fractured specimens (The first specimen to the left was not stretched, and the remaining specimens were stretched under low temperature.)

Fig. 3 Details of the tensile tests

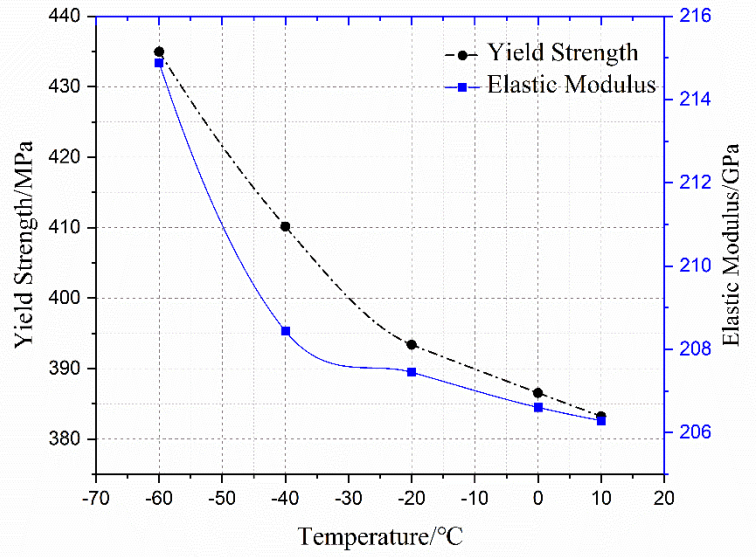

Fig. 4 The material parameters of DH36 steel at low temperatures

3. Fatigue crack propagation tests

3.1 Design of the specimens

The sampling direction coincided with the rolling direction of the steel plate so as to ensure the same mechanical properties as for that direction, see Fig. 5(a).

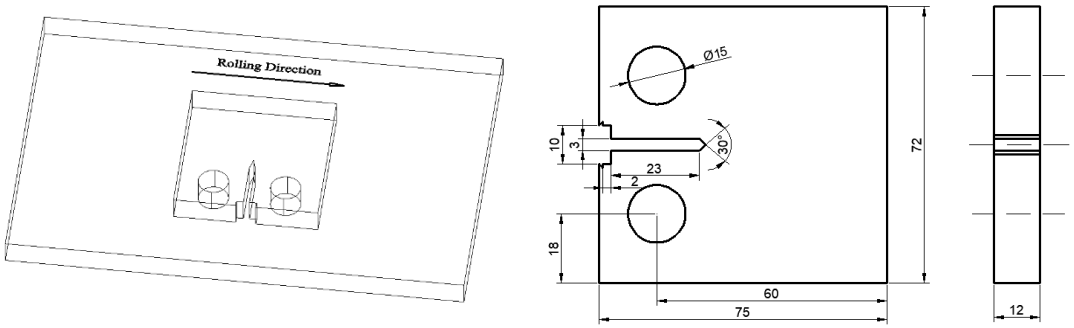

(a)Preparation of the specimen (b)The base metal specimen

Fig. 5 The specimens for the fatigue crack propagation tests

Design of the specimen was made according to ASTM E647-15 for the fatigue crack propagation test [16]. Fig. 5(b) shows the relevant dimensions of the specimen.

3.2 Crack prefabrication

Prior to the low temperature crack propagation test, cracks were prefabricated

according to ASTM E647-15 [16]. The purpose of precracking is to provide a sharpened fatigue crack of adequate size and regularity which ensures that

1) the effect of the machined starter notch is removed from the specimen *K*-calibration.

2) the effects on subsequent crack growth rate data caused by a changing shape of the crack front or the load history prior to crack formation are eliminated.

3.3 Load

The tests were carried out at -60℃~20℃. The temperature level was controlled by means of a low temperature environmental chamber (Fig. 6(a)), within which the temperature variation (inhomogeneity) was no more than 2℃, and with a PWS-250 fatigue machine as the loading equipment. The specimen was rigidly clamped at one end and loaded at the other, as shown in Fig. 6(b). The test applied a sinusoidal dynamic load with a maximum value of 15kN and a minium value of 1.5kN (which corresponds to a stress ratio of 0.1) and with a loading frequency of 10Hz.

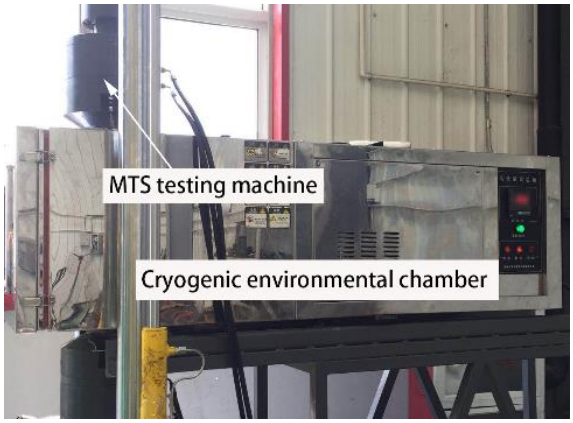

(a)Testing scene

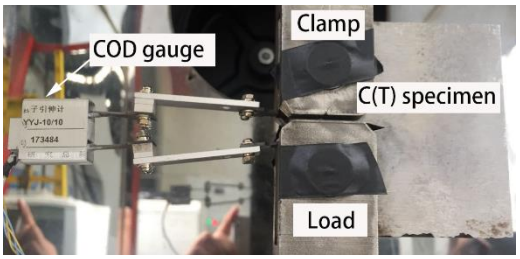

(b)Details of the environmental chamber

Fig. 6 Low temperature experimental setup of the fatigue crack propagation test

3.4 Measurement of crack length and data processing

In the fatigue crack propagation tests, the crack length is determined by means of the compliance method [16], as shown in Equations (1) and (2). A low temperature dedicated displacement gauge was placed in order to monitor the displacement,

allowing to measure the crack size.

$$U_0 = \left\{ \left[\frac{BEV_0}{P} \right]^{1/2} + 1 \right\}^{-1} \quad (1)$$

where,

U_0 is the compliance at the measuring point,

B is the thickness of the specimen,

E is the elastic modulus,

V_0 is the displacement measured by the displacement gauge,

P is the load.

The relationship between compliance and normalized crack length is shown in Equation (2).

$$a/W = 1.001 - 4.6695U_0 + 18.46U_0^2 - 236.82U_0^3 + 1214.9U_0^4 - 2143.6U_0^5 \quad (2)$$

where,

a is the length of the crack,

W is the width of the specimen.

The combination of Equations (1) and (2) indicates that change of the elastic modulus E affects the crack length a. In addition, as seen in section 2, the elastic modulus of DH36 steel varies as a function of the temperature. Therefore, the effect of the elastic modulus on the crack propagation rate was considered in this paper. The a-V_0 curves at 5 test temperatures are plotted in of Fig. 7(a). It is clear that the a-V_0 curve at -60℃ is located above the other four curves for which only minor differences are observed. The crack length corresponding to V_0=0.1mm decreases as the temperature increases, as shown in Fig. 7(b). Taking the variation of the elastic modulus with temperature into consideration, it is found that the variation of crack length is consistent with the variation of the elastic modulus at low temperatures.

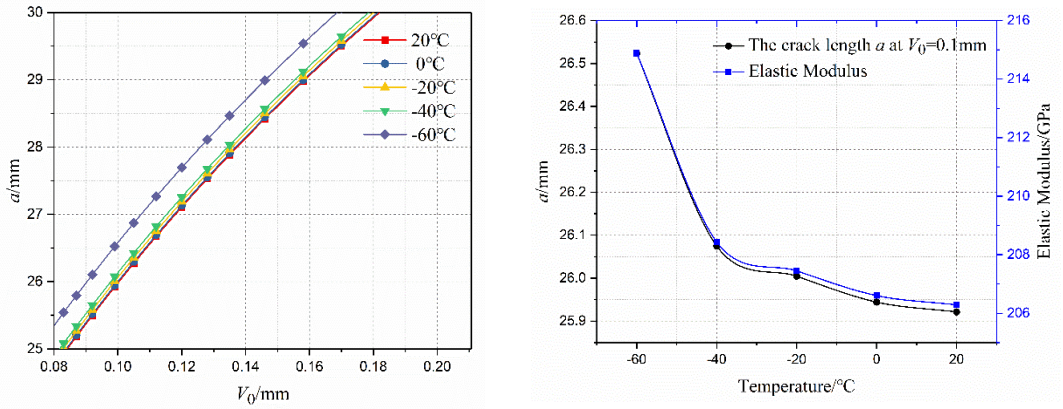

(a) The a-V_0 curve at low temperatures (b) The crack length at V_0=0.1 mm

Fig. 7 The effect of low temperatures on the a-V_0 curve

In order to obtain accurate results, the $a-N$ relationship measured by the test was processed using a 7-point incremental polynomial method. Paris pointed out that the stress intensity factor ΔK is the main parameter controlling the fatigue crack propagation rate and provided an Equation describing the fatigue crack propagation rate [16], as shown in Equation (3).

$$da/dN = C(\Delta K)^m \tag{3}$$

$$\Delta K = \left[\Delta P/B\sqrt{W}\right]\cdot\left[(2+\alpha)/(1-\alpha)^{3/2}\right]\cdot(0.886+4.64\alpha-13.32\alpha^2+14.72\alpha^3-5.6\alpha^4) \tag{4}$$

where,

N is the number of cycles,

da/dN is the fatigue crack propagation rate,

C , m are crack propagation parameters, determined by tests,

ΔK is the stress intensity factor range,

ΔP is the load range ,

α is the crack depth ratio a/W .

Taking the logarithm of both sides of Equation (3), we obtain

$$\lg(da/dN) = \lg C + m\lg(\Delta K) \tag{5}$$

It can be seen that there is a linear relationship between $\lg(da/dN)$ and $\lg(\Delta K)$, and accordingly linear regression is performed on the data by means of the least squares method. Based on this linear regression, the quantities lg$C$ and m can be

obtained [17].

4. Result and discussion

4.1 Characterization of microstructure

An optical microscope was employed in order to reveal the microstructure of DH36 steel. The base metal mainly consists of flaky pearlite and quasi-polygonal ferrite, as shown in Fig. 8.

Pearlite is a mechanical mixture at a certain mass ratio of ferrite and cementite. The mass fraction of cementite to ferrite is 12% to 88%. In the flaky pearlite, the cementite is narrow and the ferrite is broad. The mechanical properties of flaky pearlite are somewhere between those of ferrite and cementite. This implies that its strength and hardness are significantly higher than that of ferrite. The plasticity and toughness properties are worse than ferrite, but much better than cementite [18].

Ferrite is a solid solution in which carbon and an alloying element are dissolved in α-Fe. The ferrite has good ductility and toughness properties while it is also characterized by low strength and hardness.

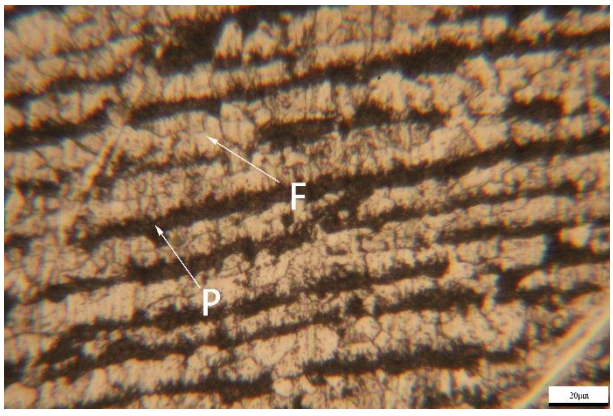

Fig. 8 The microstructure of DH36 steel

4.2 Fatigue crack propagation rate

Fig. 9(a) shows the variation of the fatigue crack propagation rate at temperatures in the range from -60℃ to 20℃ for DH36 steel. Fig. 9(a) shows minor differences of fatigue propagation rates for different temperatures in the low ΔK range. As ΔK

increases, the fatigue crack propagation rate increases for increasing temperatures.

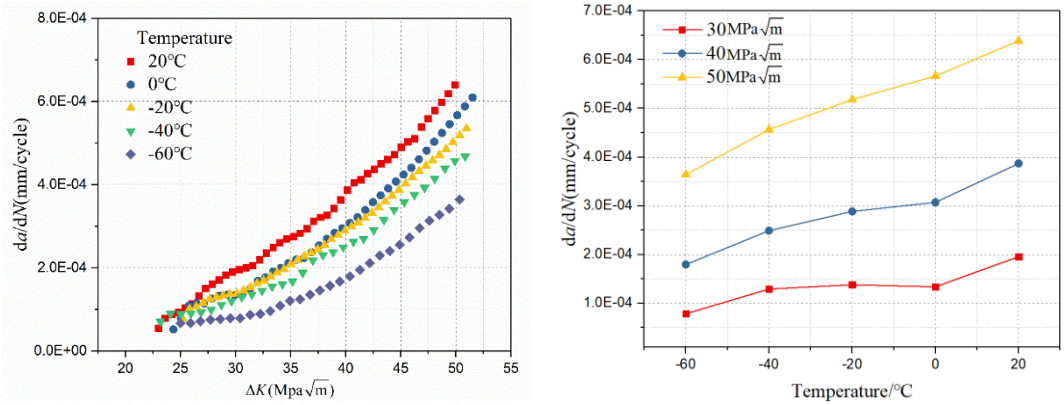

(a) The fatigue crack propagation rates at different temperatures

(b) The fatigue crack propagation rates for different ΔK

Fig. 9 The results of the fatigue crack propagation tests

As the temperature increases, the fatigue crack propagation rates increase for a given value of ΔK, as shown in Fig. 9(b). The fatigue crack propagation rates increase slowly for increasing temperatures when $\Delta K = 30\text{MPa}\sqrt{\text{m}}$. In particular, the fatigue crack propagation rates in the temperature range from t -40℃ to 0℃ are not significantly different. When $\Delta K = 40\text{MPa}\sqrt{\text{m}}$, the differences between fatigue crack propagation rates for different temperatures become larger. When $\Delta K = 50\text{MPa}\sqrt{\text{m}}$, the fatigue crack propagation rates grow rapidly for increasing temperatures.

Table 3 Fitting parameters at different temperatures

Temperature/℃	Stress ratio	Frequency/Hz	lg$C$	m	R^2
20	0.1	10	-7.649	2.633	0.981
0	0.1	10	-7.639	2.571	0.990
-20	0.1	10	-7.492	2.469	0.998
-40	0.1	10	-7.709	2.568	0.996
-60	0.1	10	-8.130	2.740	0.978

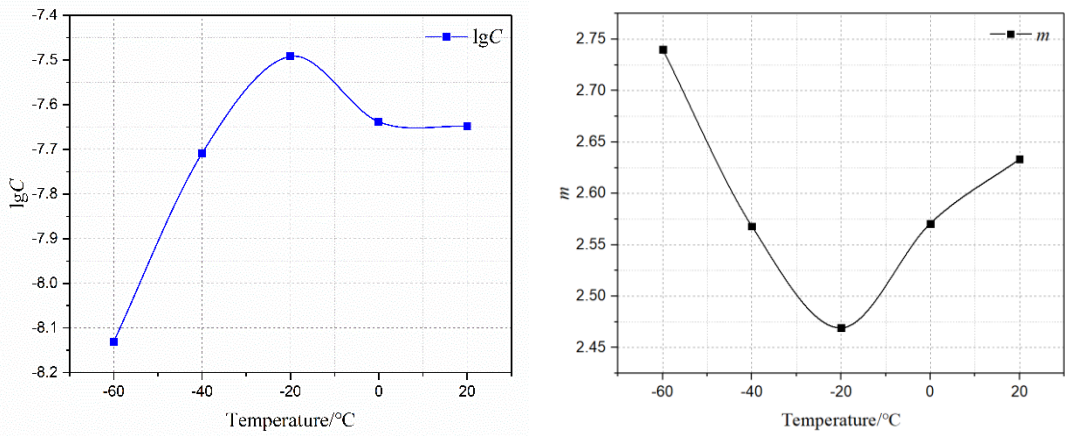

(a)lg$C$ (b)m

Fig. 10 Paris law propagation parameters at low temperatures

The parameters of the Paris propagation law are given in Table 3 based on fitting the data by Equation(1) for the stable crack propagation phase. The regression coefficient corresponding to the fitted curve exceeds 0.95, which represents a high level of correlation between the fatigue data and the curve which represents Paris law. The relationships between lg$C$, m and temperature in Table 3 are plotted as curves in Fig. 10 It is seen that the m value decreases and lg$C$ increases from -60℃ to -20℃, while from -20℃ to 20℃, there is a reversed trend for the variation of m and lg$C$. The trends for m and lg$C$ in this paper are consistent with the study of Liao [10].

Jung [19] has summarized several mechanisms responsible for the fatigue crack propagation behavior, including the deformation-induced martensitic transformation, the crack closure effect on the near-threshold fatigue crack propagation, the Fatigue Ductile to Brittle Transition, and thermal activation based on the dislocation dynamics concept. In this paper, the fatigue crack propagation rate for the base metal subjected to decreasing temperatures may be strongly connected to the change of fracture mode, namely the Fatigue Ductile to Brittle Transition. The relevant details are discussed in subsequent chapter.

4.3 Failure modes

The fractography of the specimens was studied by means of a Scanning Electron Microscope (SEM) in order to determine the failure modes and the effects of

temperature level. Three different zones that correspond to different values of ΔK can clearly be observed. These are the crack initiation zone, the stable growth zone, and the instantaneous fracture zone [20], and these are shown in Figure 11 for different temperature levels.

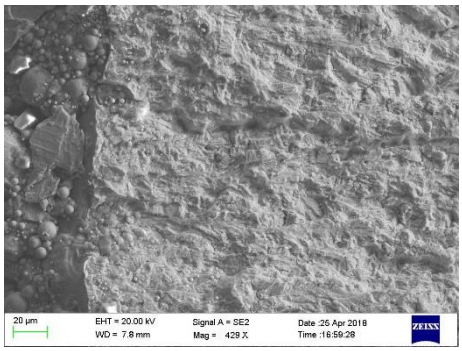

(a) The crack initiation zone of the base metal at 20℃

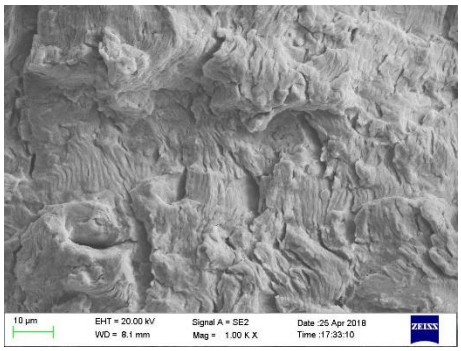

(b) Stable growth zone of the base metal at 20℃ ($\Delta K = 30\text{MPa}\sqrt{\text{m}}$)

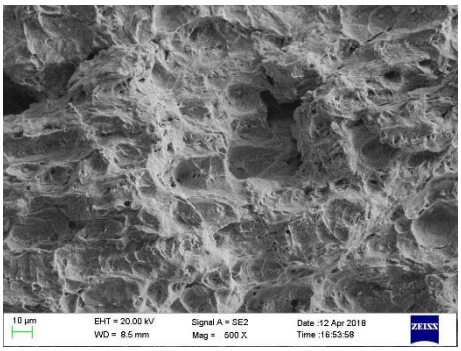

(c) Instantaneous fracture zone of the base metal at 20℃

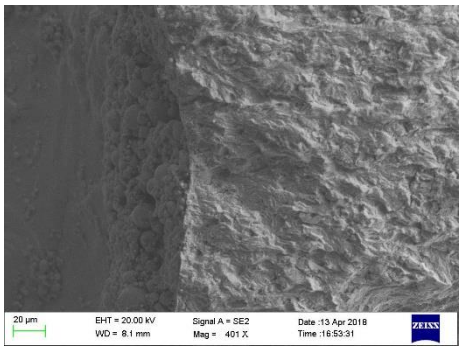

(d) The crack initiation zone of the base metal at 0℃

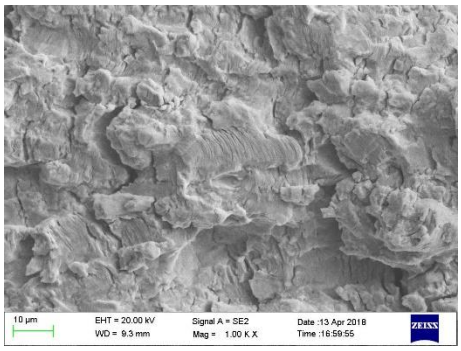

(e) Stable growth zone of the base metal at 0℃ ($\Delta K = 30\text{MPa}\sqrt{\text{m}}$)

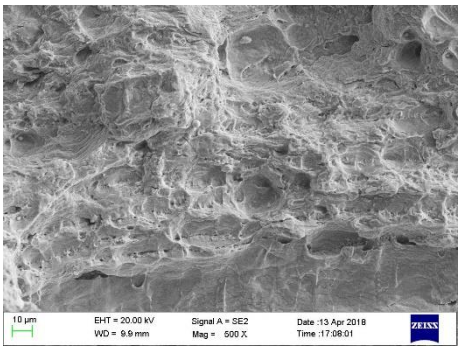

(f) Instantaneous fracture zone of the base metal at 0℃

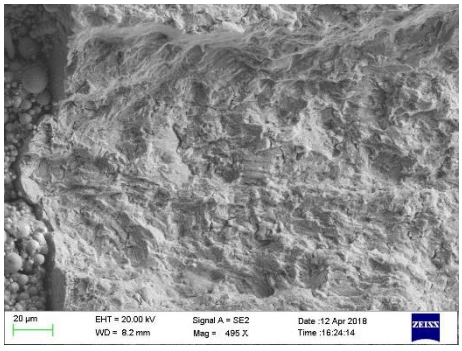

(g) The crack initiation zone of the base metal at -20℃

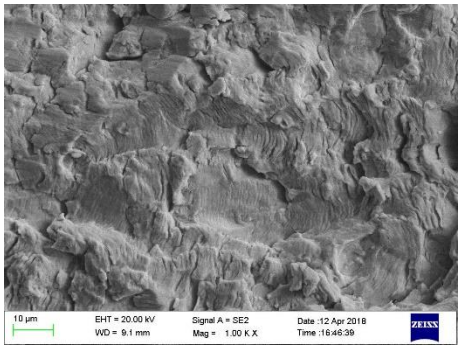

(h) Stable growth zone of the base metal at -20℃ ($\Delta K = 30\text{MPa}\sqrt{\text{m}}$)

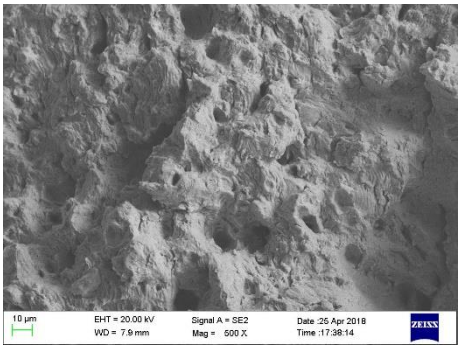

(i) Instantaneous fracture zone of the base metal at -20℃

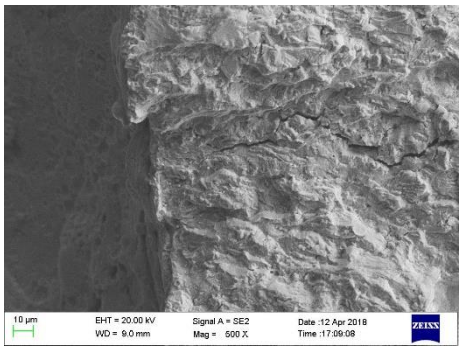

(j) The crack initiation zone of the base metal at -40℃

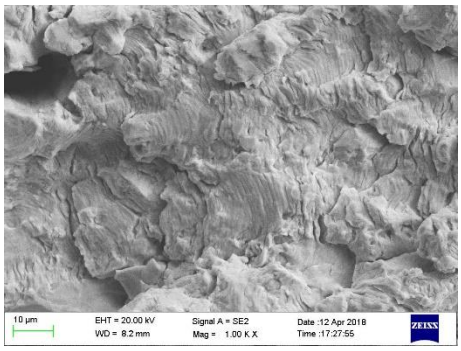

(k) Stable growth zone of the base metal at -40℃ ($\Delta K = 30\text{MPa}\sqrt{\text{m}}$)

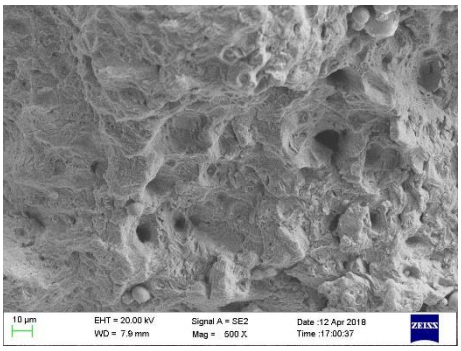

(l) Instantaneous fracture zone of the base metal at -40℃

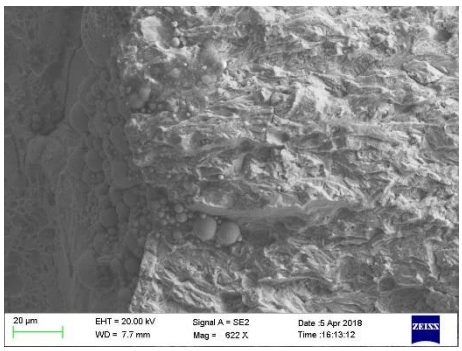

(m) The crack initiation zone of the base metal at -60℃

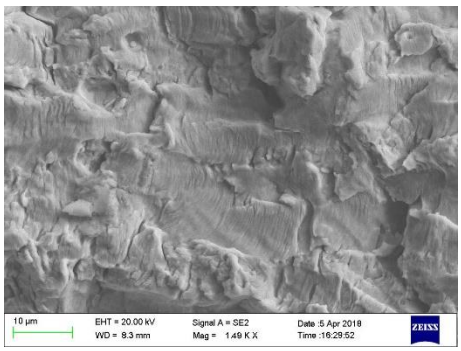

(n) Stable growth zone of the base metal at -60℃ ($\Delta K = 30\text{MPa}\sqrt{\text{m}}$)

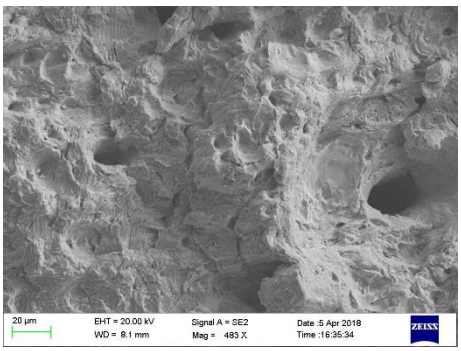

(o) Instantaneous fracture zone of the base metal at -60℃

Fig. 11 The fractured surface microstructure for C(T) specimens at -60℃~20℃

In the low ΔK range， the crack is at the initiation stage [21], and as the temperature is reduced , the number of potential crack sources is reduced, as shown in Fig. 11(a, d, g, j, m). As the stress intensity factor increases, a dominant growing crack is initiated at a certain defect and this represents the main crack. The low temperature fracture of specimens which are previously subjected to cyclic loads in the crack initiation zone shows an increase in the number of cleavage facets with a tongue pattern, which are often orthogonal to each other. The existence of a large number of tongue patterns suggests that twinning has developed, and hence impeded the slip.

For the medium ΔK range, the crack is in the stable growth zone, and clear fatigue striations can be observed as part of the fracture topography. According to the "plastic passivation model" proposed by Laird [22], the growth of each crack passes through the processes of "opening, passivation, expansion, sharpening" , which corresponds to a

stress cycle that leaves a trace called a "fatigue striation" on the crack surface. Therefore, a fatigue striation marks the completion of a stress cycle, and the spacing of the fatigue striations represent the distance corresponding to the crack propagation caused by the stress cycle, i.e. reflecting the fatigue crack propagation rates [23]. As seen from Fig. 11(b, e, h, k, n), as the temperature is lowered, the spacing of the fatigue striations gradually narrows. This means that given $\Delta K = 30\text{MPa}\sqrt{\text{m}}$, the fatigue crack propagation rate decreases as the temperature decreases.

In the high ΔK range, the crack is at the stage of instantaneous fracture, and different fracture modes are found at five temperatures. At 20°C, a distinct dimple appeared in the fracture zone (Fig.11(c)), which means that plastic fracture is taking place. As the temperature is lowered, the plasticity of DH36 steel is gradually reduced while brittleness is increased. It can be found that the dimples in the fracture are much more shallow and reduced in numbers at 0°C (Fig. 11(f)). Both shallow and small dimples and cleavage steps are observed at -20°C, which represent mixed fracture states (Fig. 11(i)). For the fractures at -40°C and -60°C, as toughness is reduced, the cleavage steps become increasingly visible while the dimples are gradually reduced (Fig. 11(l) and Fig. 11(o)). There is a remarkable morphological difference between the resulting fracture modes. This indicates that Fatigue Ductile to Brittle Transition occurs for the tested base metal C(T) specimens within the temperature range from -60°C to 20°C.

4.4 Existence of the Fatigue Ductile to Brittle Transition

A Ductile to Brittle Transition similar to that of fracture has also been documented for fatigue at low temperatures [24-26] and it has been named the Fatigue Ductile–Brittle Transition (FDBT). The temperature at which this transition occurs is known as the Fatigue Transition Temperature (FTT). It has been observed that lower temperatures generally cause reduced fatigue crack propagation rates until the FTT is reached. Below the FTT, higher fatigue crack propagation rates are encountered [27].

Review of current literature on the topic shows the influence of such low temperatures on the fatigue crack propagation behavior of metals that undergo FDBT

is the result of two competing effects [28]. On the one hand, an increase of the stress necessary for producing plastic flow is observed as the temperature is lowered: its thermal component (effective stress), which is and expression for the short range barriers that mobile dislocations must overcome [29], is inversely proportional to the temperature such that plastic deformation is hindered as temperature is decreased. On the other hand, when temperature is lowered below the steel FTT, ‘‘static’’ modes of crack propagation, such as micro cleavage cracking and micro-void coalescence, are activated.

Fractography illustrates that DH36 steel experiences FDBT within the temperature range from -60℃ to 20℃. When the fatigue crack propagation tests are performed at temperatures the FTT (near -20℃), a clear general improvement of the fatigue crack propagation curve is obtained. However, when the temperature is lowered below the FTT (in this case, T < -20℃), a ‘‘competition’’ between the two aforementioned effects appears. When the temperature drops below FTT, the favorable effects of the increased stress required to induce plastic flow becomes dominant once again, and it can be seen that the fatigue crack propagation rate continues to decrease as the temperature is lowered below -20℃.

The toughness of metals decreases with decreasing temperature, and changes from ductile fracture to brittle fracture, which is called the Ductile to Brittle Transition. The temperature at the corresponding characteristic transition point is called the Ductile to Brittle Transition Temperature. The transition temperature is also known as the cold brittle transition temperature. Mainly due to the change of the internal crystal structure of steel for changing temperatures, the toughness and brittleness of steel also changes accordingly.

Impact tests of DH36 steel under low temperature was carried out by Chen [30]. The specimen of the impact test was designed and manufactured according to GB/T 229 [31]. The notch was V-shaped, and the dimensions of the test piece were as shown in Fig. 12. The impact test was carried out at -80 ℃~0 ℃, and the temperature inhomogeneity did not exceed 2 ℃.

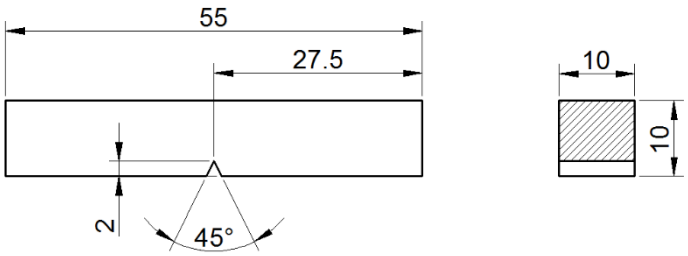

Fig. 12 The specimen of the impact test

The sample was placed between the two seats of the test machine, and the notch was placed at the reverse side of the impacted surface. The sample was hit by a pendulum and the absorbed energy of the specimen was measured. The curve representing the shock absorbed energy versus the temperature was plotted and the Ductile to Brittle Transition Temperature of the material was determined by this curve. His experimental results showed that the Ductile to Brittle Transition Temperature (DBTT) of DH36 Steel is around -50℃, while the FTT is about -20℃, which is 30℃ higher than DBTT. The fatigue crack growth performance of DH36 steel was found to change drastically at FTT. Therefore, this effect of FDBT may have serious consequences for the design and operation of civil, offshore, and marine structures.

Wallin [32] proposed the following relationship between the transition temperatures of fracture and Charpy impact energy, as shown in Equation (6).

$$T_0 = T_{27J} - 18℃ \pm 15℃ \tag{6}$$

Where,

T_0 is the temperature at which K_{Ic} is $100\text{MPa}\sqrt{\text{m}}$,

T_{27J} is the temperature at which the Charpy impact energy is 27J (℃),

K_{IC} is critical stress intensity factor for mode I ($\text{MPa}\sqrt{\text{m}}$).

Walters estimate that the FTT is approximately 36 ℃ higher than T_0, and the FTT should then be approximately 18 ℃ higher than T_{27J} [28]. Based on that study, the FTT can be estimated by means of the Charpy impact test. The relationship between FTT and DBTT also matches the findings of the present paper.

In the design process of the structure, the ambient temperature should stay above the FTT of the material. However, there are few studies in relation to the FTT of metallic

materials, let alone FTT data. It is recommended that more materials, including welds and base metals, should be considered in the future.

5. Conclusion

The objective of the present paper is to investigate the fatigue crack propagation behavior of DH36 steel at low temperatures by carrying out tensile tests and fatigue crack propagation tests of DH36 steel for such temperatures. The above investigation leads to the following conclusions:

1） The fatigue crack propagation rate decreases with decreasing temperature, and the crack growth parameter *m* decreases while the parameter lg*C* increases from -60℃ to -20℃, while from -20℃ to 20℃, there is a reversed trend for the variation of *m* and lg*C*.

2） FDBT of DH36 steel occurred within the temperature range from f -60℃ to20℃, the FTT of DH36 steel is around -20℃, which is higher than that of DBTT. Consequently, prevention of FDBT will be of main concern for practicing engineers.

3） The relationship between FDBT and DBTT is currently not clearly defined. The FTT obtained by DBTT estimation is in a fuzzy range. A clear relationship and the internal mechanisms associated with the two phenomena should be the subject of future studies.

Acknowledgements

This paper was supported by the National Natural Science Foundation, Fund No. 51679050, China.

Reference

1. Fricke W, von Lilienfeld-Toal A, et al. Fatigue strength investigations of welded details of stiffened plate structures in steel ships. *International Journal of Fatigue.* 2012;34(1):17-26.
2. Zhang HX, Wei CY, et al. Research on fatigue crack propagation behaviour of 4003 ferritic stainless steel based on infrared thermography. *Fatigue & Fracture*

of Engineering Materials & Structures. 2016;39(2):206-216.
3. Yan X, Huang X, et al. Prediction of fatigue crack growth in a ship detail under wave-induced loading. *Ocean Engineering.* 2016;113:246-254.
4. Josefson BL, Ringsberg JW. Assessment of uncertainties in life prediction of fatigue crack initiation and propagation in welded rails. *International Journal of Fatigue.* 2009;31(8-9):1413-1421.
5. Kiss K, Dunai L. Fracture mechanics based fatigue analysis of steel bridge decks by two-level cracked models. *Computers & Structures.* 2002;80(27):2321-2331.
6. Pipinato A, Pellegrino C, et al. Fatigue assessment of highway steel bridges in presence of seismic loading. *Engineering Structures.* 2011;33(1):202-209.
7. Suh CM, Suh MS, et al. Growth behaviour of small surface fatigue cracks in AISI 304 stainless steel. *Fatigue & Fracture of Engineering Materials & Structures.* 2012;35(1):22-29.
8. Albuquerque C, Silva ALL, et al. An efficient methodology for fatigue damage assessment of bridge details using modal superposition of stress intensity factors. *International Journal of Fatigue.* 2015;81:61-77.
9. Qian X, Nguyen CT, et al. Fatigue performance of tubular X-joints with PJP+ welds: II — Numerical investigation. *Journal of Constructional Steel Research.* 2013;89:252-261.
10. Liao XW, Wang YQ, et al. Fatigue crack propagation for Q345qD bridge steel and its butt welds at low temperatures. *Fatigue & Fracture of Engineering Materials & Structures.* 2018;41(3):675-687.
11. Jeong D, Sung H, et al. Fatigue crack propagation behavior of Fe25Mn and Fe16Mn2Al steels at room and cryogenic temperatures. *Metals and Materials International.* 2016;22(4):601-608.
12. Fassina P, Brunella MF, et al. Effect of hydrogen and low temperature on fatigue crack growth of pipeline steels. *Engineering Fracture Mechanics.* 2013;103:10-25.
13. CCS. Rules for classification of sea-going steel ships. In:2006.
14. DNVGL. Rules for Classification of ships new building. In:2017.
15. GB/T. Metal material-tensile testing at low temperature. In:2006.
16. ASTM. Standard test method for measurement of fatigue crack growth rates. In. Vol E647-152015.
17. Antunes F, Prates P, et al. Elastic correction of fatigue crack growth laws. *Fatigue & Fracture of Engineering Materials & Structures.* 2019;42(5):1052-1061.
18. Yuan H, Zhang W, et al. Microstructure-sensitive estimation of small fatigue crack growth in bridge steel welds. *International Journal of Fatigue.* 2018;112:183-197.
19. Jung D-H, Kwon J-K, et al. S–N Fatigue and Fatigue Crack Propagation Behaviors of X80 Steel at Room and Low Temperatures. *Metallurgical and Materials Transactions A.* 2013;45(2):654-662.
20. Benedetti M, Fontanari V, et al. Crack growth resistance of MAG butt-welded

joints of S355JR construction steel. *Engineering Fracture Mechanics.* 2013;108:305-315.
21. Gerberich W.W, Yu W, et al. Fatigue Threshold Studies in Fe, Fe-Si, and HSLA Steel: Part I1. Thermally Activated Behavior of the Effective Stress Intensity at Threshold. *METALLURGICAL TRANSACTIONS A.* 1983;15A.
22. Laird C, Krause AR. A theory of crack nucleation in high strain fatigue. *International Journal of Fracture.* 1968;4:219-231.
23. Richter-Trummer V, R.M.C.Miranda, Albuquerque C. Fatigue Crack Striation Spacing for Welded and Base Material CT Steel Specimens. *ADVANCED MATERIALS FORUM VI, PTS 1 AND 2.* 2013;730-732:793.
24. Xiuli LBaZ. Predicting fatigue crack initiation life of an aluminium alloy at low temperatures. *Fatigue Fract Engng Muter Struct.* 1992;15(12):1213-1221.
25. Moody NR, Gerberich WW. Fatigue crack propagation in iron and two iron binary alloys at low temperatures. *Materials Science and Engineering.* 1979;41(2):271-280.
26. Verkin BI, Grinberg NM, et al. Low temperature fatigue fracture of metals and alloys. *Materials Science and Engineering.* 1983;58(2):145-168.
27. Walters CL. The Effect of Low Temperatures on the Fatigue of High-strength Structural Grade Steels. *Procedia Materials Science.* 2014;3:209-214.
28. Walters CL, Alvaro A, et al. The effect of low temperatures on the fatigue crack growth of S460 structural steel. *International Journal of Fatigue.* 2016;82:110-118.
29. Majzoobi GH, Mahmoudi AH, et al. Ductile to brittle failure transition of HSLA-100 Steel at high strain rates and subzero temperatures. *Engineering Fracture Mechanics.* 2016;158:179-193.
30. Chen F. Development and production of DH36 jacket platform steel plate. *Shandong Metallurgy.* 2014;38:7-9.
31. Qiuli Z, Hong S, et al. GB / T229-2007 Metallic materials-Charpy pendulum impact test method. 2010(3):190-192.
32. K W. A Simple Theoretical Charpy-V – KIc correlation for irradiation embrittlement. *ASME-PVP.* 1989;170:93-100.